Journal of Nuclear Materials 381 (2008) 46–54

Contents lists available at ScienceDirect

Journal of Nuclear Materials

journal homepage: www.elsevier.com/locate/jnucmat

Irradiation induced creep behavior of H-451 graphite

Timothy D. Burchell

Materials Science and Technology Division, Oak Ridge National Laboratory, P.O. Box 2008, Oak Ridge, TN 37831-6088, USA

A B S T R A C T

The application of a creep model previously applied to compressive creep data for H-451 irradiated at 900 °C (13.7 and 20.8 MPa) has been extended to compressive creep data for H-451 irradiated at 600 °C (13.7 and 20.8 MPa). The basis of the creep model is discussed and the experimental data required to evaluate the terms in the creep model are reported and discussed. The model, which corrects the true (crystal) creep strain for the effect of creep on the dimensional change component of the creep specimen, is shown to be a good fit to the data. Creep strain data for H-451 graphite irradiated at 900 °C under a tensile stress of 6 MPa are also reported, along with the required experimental data to evaluate the terms in the creep model. The model is shown to inadequately represent the high dose (post volume turnaround) H-451 tensile creep strain data. Reasons for the models limitation are discussed and an approach to a potentially improved graphite irradiation creep model is suggested.

1. Introduction

The US Department of Energy is planning the construction of a Very High Temperature Reactor (VHTR), named the Next Generation Nuclear Plant (NGNP). The NGNP is a graphite-moderated, helium cooled rector capable of providing high temperature process heat and electricity. Graphite irradiation induced creep data are needed for NGNP design and licensing purposes. Consequently, new irradiation creep experiments are being planned and designed to furnish the required data [1,2]. In a parallel effort compressive creep data for grade H-451 graphite is being re-analyzed and previously unpublished data for the high dose tensile creep behavior of H-451 are analyzed and reported.

During operation in the reactor core graphite undergoes neutron irradiation induced dimensional changes [3,4]. Local differences in neutron dose and temperature cause differential stresses to develop in the graphite. These stresses are relaxed by neutron irradiation induced creep strain. Graphite does not undergo thermal creep at the temperatures experienced in the reactor core. The irradiation induced creep strains in graphite can be very large, exceeding several percent, and premature failure of the graphite would occur if it were not for irradiation induced creep strain.

A mechanism for the irradiation induced creep of graphite has been proposed by Kelly and Foreman [5] which involves irradiation induced basal plane dislocation pinning/unpinning in the graphite crystals. Pinning sites are created and destroyed by neutron irradiation (radiation annealing). Under neutron irradiation dislocation lines may be completely or partially pinned depending upon the dose and temperature of irradiation. The pinning points were speculated to be interstitial atom clusters 4 ± 2 atoms in size [6,7]. The interstitial clusters are temporary barriers since they are annealed (destroyed) by further irradiation. Thus irradiation can release dislocation lines from their original pinning site and the crystal can flow due to basal plane slip at a rate determined by pinning and unpinning of dislocations.

Kelly and Foreman's theory assumes that polycrystalline graphite consists of a single phase of true density ρ_0 and apparent density ρ. The material may be divided into elementary regions in which the stress may be considered uniform and which may be identified as mono-crystalline graphite. Significantly, the model excludes porosity. It is further assumed that the only deformation mode is basal plane slip for which the strain rate is determined by

$$\dot{\varepsilon}_{xz} = k(\sigma_{xz})\gamma, \quad \text{and} \tag{1}$$

$$\dot{\varepsilon}_{yz} = k(\sigma_{yz})\gamma, \tag{2}$$

where γ is the fast neutron flux, k is the steady state creep coefficient, and σ is the stress in the given direction. The microscopic deformation assumes the usual relationship between the basal plane shear rate ($\dot{\varepsilon}$) and the mobile dislocation density (Ω), and is given by

$$\dot{\varepsilon} = \Omega b v = k\sigma\gamma, \tag{3}$$

where b is the Burgess vector and v is the dislocation velocity as a function of the pinning point concentration in the basal plane as the pins are created and destroyed by neutron flux. The dislocation line flow model used the flexible line approach where the dislocation line is pinned/unpinned and the dislocation line bowing is a function of the line tension and pin spacing. The concentration of pinning sites increases under irradiation from the initial value (from intrinsic defects) to a steady state concentration. The initial creep rate is high and decreases to a steady state value as the pinning

E-mail address: burchelltd@ornl.gov

0022-3115/$ - see front matter © 2008 Elsevier B.V. All rights reserved.
doi:10.1016/j.jnucmat.2008.07.022

concentration saturates at a level controlled by the neutron flux and temperature. Thus a two-stage model can be envisioned where the primary creep rate is initially high and falls to a secondary or 'steady state' creep rate. The steady state creep term should be dominated by the dose at which physical property changes due to dislocation pinning have saturated. Kelly and Foreman state that at higher temperatures the steady state (secondary) creep rate (k) would be expected to increase due to (i) incompatibility of crystal strains increasing the internal stress and thus enhancing the creep rate, and (ii) additional effects due to the destruction of interstitial pins by thermal diffusion of vacancies (thermal annealing as well as irradiation annealing). Kelly and Foreman [5] further speculate that the non-linearity of creep strain with stress, which is expected at higher stress levels, may also be related to the high dose dimensional change behavior of polycrystalline graphite [8].

The apparent (experimentally determined) irradiation creep strain is conventionally defined as the difference in dimensional changes between a stressed sample and an unstressed sample irradiated under identical conditions. Early creep data [9–14] was observed to fit a two-stage simple visco-elastic model where the total creep strain was comprised of a reversible primary creep plus a secondary or steady state creep proportional to the applied stress and the neutron dose (as described above for the dislocation pinning/unpinning model). The magnitude of the total primary creep strain was observed to be approximately equal to one elastic strain unit (σ/E_0), where σ is the applied stress and E_0 is the unirradiated static Young's modulus appropriate to the level of the applied stress. The steady state (secondary) creep was shown to be represented by a linear law such that the total irradiation creep strain is given by

Total irradiation creep (ε_c) = Primary (transient) creep + Secondary (steady state) creep

$$\varepsilon_c = \frac{a\sigma}{E_0}[1 - \exp(-b\gamma)] + k\sigma\gamma, \tag{4}$$

where ε_c is the total (apparent) creep strain, σ *is the* applied uniaxial stress, E_0 is the initial (preirradiated) Young's modulus, and γ *is the* fast neutron fluence.a and b are constants (a is usually = 1), and k is the steady state creep coefficient in units of reciprocal neutron dose and reciprocal stress. Because the primary creep saturates at very low doses (<10^{20} n/cm^2 [E > 50 keV]) to approximately one elastic strain (σ/E_0) the total creep may be represented as

$$\varepsilon_c = \frac{\sigma}{E_0} + k\sigma\gamma. \tag{5}$$

In the UK the total creep strain is often normalized to the initial elastic strain and written as

$$\varepsilon_c = 1 + kE_0\gamma, \tag{6}$$

in elastic strain units (esu), or creep strain per unit initial elastic strain, where kE_0 is the creep coefficient in units of reciprocal dose.

The creep coefficient, k, was found to be independent of the sign of the applied stress, and the linear visco-elastic law was found to be a good fit to low and intermediate dose creep strain data [11,15,16]. However, as increasingly larger creep strain data and neutron dose data became available a marked deviation from the linear law was observed [17,18]. Several models have been advanced to explain this deviation from linearity and better represent the data. For example, the UK creep law [17,18] recognizes that the initial creep coefficient, k, is modified by irradiation induced structure changes. Hence total creep strain is given by

$$\varepsilon_c = \frac{\sigma}{E_0} + \left(\frac{d\varepsilon_c}{d\gamma}\right)_0 \sigma \int_0^\gamma S^{-1}(\gamma)\cdot d\gamma, \tag{7}$$

where σ *is the* applied uniaxial stress, $(d\varepsilon/d\gamma)_0$ is the initial secondary creep rate (k_0), γ is the fast neutron fluence, and $S(\gamma)$ is the structure factor, given by, $S(\gamma)$ is the E/E_p the ratio of the Young's modulus at dose γ to the Young's modulus after the initial increase due to dislocation pinning.

In a reevaluation of the UK creep data Kelly and Brocklehurst [17,18] developed a creep model that took into account the structural changes that occur in the graphite as a consequence of creep, and that manifest themselves as changes in the coefficient of thermal expansion (CTE). Kelly and Burchell [19] showed that the application of this model to grade H-451 graphite irradiation creep data at 900 °C to doses of ~0.5×10^{22} n/cm^2 [E > 50 keV] or ~3.4 displacements per atom (dpa) gave good agreement with the experimental (apparent) creep strain data. Here we demonstrate the applicability of the Kelly and Burchell model [19] for H-451 creep strain data at an irradiation temperature of 600 °C to a dose of ~0.5×10^{22} n/cm^2 [E > 50 keV] or ~3.4 dpa. Furthermore, the model is tested against H-451 tensile creep strain data from irradiation experiments at 900 °C to a dose of ~2×10^{22} n/cm^2 [E > 50 keV] or 13.6 dpa. Deficiencies in the model as applied to high neutron dose creep strain data are reported and discussed.

2. Theory

The Kelly and Burchell [19] model recognizes that creep produces significant modifications to the dimensional change component of the stressed specimen compared to that of the control and that this must be accounted for in the correct evaluation of creep strain data.

The rate of change of dimensions with respect to neutron dose γ (n/cm^2) in appropriate units is given by the Simmons' theory [20] for direction x in the unstressed polycrystalline graphite

$$g_x = \left(\frac{\alpha_x - \alpha_a}{\alpha_c - \alpha_a}\right)\left(\frac{dX_T}{d\gamma}\right) + \frac{1}{X_a}\cdot\frac{dX_a}{d\gamma} + F_x, \tag{8}$$

where α_x is the thermal expansion coefficient in the x-direction, α_c and α_a are the thermal expansion coefficients of the graphite crystal parallel and perpendicular to the hexagonal axis, respectively, over the same temperature range. The term F_x is a pore generation term that becomes significant at intermediate doses when incompatibilities of irradiation induced crystal strains cause cracking of the bulk graphite [21]. For the purposes of this analysis the term F_x is ignored. The parameters $(1/X_c)(dX_c/d\gamma)$ and $(1/X_a)(dX_a/d\gamma)$ are the rates of change of graphite crystallite dimensions parallel and perpendicular to the hexagonal axis, and

$$\frac{dX_T}{d\gamma} = \frac{1}{X_c}\cdot\frac{dX_c}{d\gamma} - \frac{1}{X_a}\cdot\frac{dX_a}{d\gamma}. \tag{9}$$

The imposition of a creep strain is known to change the thermal expansion coefficient of a stressed specimen, increasing it for a compressive strain and decreasing it for a tensile strain compared to an unstressed control. Thus, the dimensional change component of a stressed specimen at dose γ (n/cm^2) is given by

$$g'_x = \left(\frac{\alpha'_x - \alpha_a}{\alpha_c - \alpha_a}\right)\left(\frac{dX_T}{d\gamma}\right) + \frac{1}{X_a}\cdot\frac{dX_a}{d\gamma} + F'_x, \tag{10}$$

where α'_x is the thermal expansion coefficient of the crept sample, and F'_x is the pore generation term for the crept specimen. The difference between these two equations is thus the dimensional change correction that should be applied to the apparent creep strain (the pore generation terms F_x and F'_x are neglected)

$$\begin{aligned} g'_x - g_x &= \left(\frac{\alpha'_x - \alpha_a}{\alpha_c - \alpha_a}\right)\left(\frac{dX_T}{d\gamma}\right) - \left(\frac{\alpha_x - \alpha_a}{\alpha_c - \alpha_a}\right)\left(\frac{dX_T}{d\gamma}\right) \\ &= \left(\frac{\alpha'_x - \alpha_x}{\alpha_c - \alpha_a}\right)\left(\frac{dX_T}{d\gamma}\right). \end{aligned} \tag{11}$$

The true creep strain rate can now be expressed as

$$\frac{d\varepsilon}{d\gamma} = \frac{d\varepsilon'}{d\gamma} - \left(\frac{\alpha'_x - \alpha_x}{\alpha_c - \alpha_a}\right)\left(\frac{dX_T}{d\gamma}\right), \tag{12}$$

where ε is the true creep strain and ε' is the apparent creep strain determined experimentally in the conventional manner.

Thus the true creep strain (ε_c) parallel to the applied creep stress is given by

$$\varepsilon_c = \varepsilon'_c - \int_0^{\gamma}\left(\frac{\alpha'_x - \alpha_x}{\alpha_c - \alpha_a}\right)\left(\frac{dX_T}{d\gamma}\right)\cdot d\gamma, \tag{13}$$

where ε'_c is the induced apparent creep strain, $(\alpha'_x - \alpha_x)$ is the change in coefficient of thermal expansion as a function of dose, $(\alpha_c - \alpha_a)$ is the difference of the crystal thermal expansion coefficients of the graphite parallel and perpendicular to the hexagonal axis, X_T is the crystal shape change parameter given above, and γ is the neutron dose. The apparent (experimental) creep strain is thus given by

$$\varepsilon'_c = \varepsilon_c + \int_0^{\gamma}\left(\frac{\alpha'_x - \alpha_x}{\alpha_c - \alpha_a}\right)\left(\frac{dX_T}{d\gamma}\right)\cdot d\gamma. \tag{14}$$

Substituting for ε_c from Eq. (5) gives the apparent (experimental) creep strain ε'_c as

$$\varepsilon'_c = \left(\frac{\sigma}{E_0} + k\sigma\gamma\right) + \int_0^{\gamma}\left(\frac{\alpha'_x - \alpha_x}{\alpha_c - \alpha_a}\right)\left(\frac{dX_T}{d\gamma}\right)\cdot d\gamma, \tag{15}$$

with the terms as defined above.

3. Experimental

3.1. Materials

Grade H-451 is a medium grain, near-isotropic, extruded nuclear grade graphite. The bulk density is ~1.75 g/cm^3 and the mean grain size is 0.5 mm. The microstructure of H-451 is illustrated in Fig. 1.

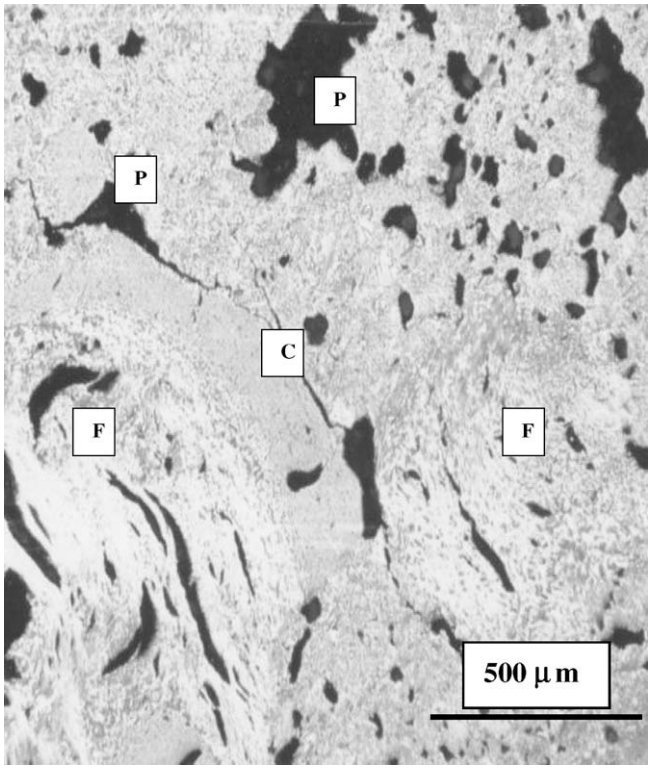

Fig. 1. An optical photomicrograph of the microstructure of grade H-451 graphite revealing the presence of pores [P], coke filler particles [F] and cracks [C].

3.2. Creep capsules

A series of compressive creep capsules were irradiated in the Oak Ridge Research Reactor (ORR) [22] in the late 1970s. Compressive creep stresses of 13.8 and 20.7 MPa (2 ksi and 3 ksi, respectively) were applied at irradiation temperatures of 600 and 900 °C. The peak neutron dose was ~0.5×10^{22} n/cm^2 [E > 50 keV], or ~3.4 dpa. The capsule was heated electrically and fully thermocoupled. The creep stress was applied using gas filled bellows and measured with an in-situ load cell. The capsules contained both stressed and unstressed H-451 samples with nominal dimensions of 12.7 mm diameter and 25.4 mm length. The majority of the creep and control specimens were machined with their major axis parallel to the extrusion direction, or with grain (WG). However, a limited number where cut in the perpendicular to extrusion direction, or against grain (AG) [23].

Tensile creep experiments [24,25] were conducted in the high flux reactor (HFR) at Joint Research Center, Petten, The Netherlands. H-451 specimens were irradiated to a peak dose of ~2×10^{22} n/cm^2 [E > 50 keV] or 13.6 dpa at a temperature of ~900 °C under an applied tensile stress of 6 MPa. All the tensile creep and control specimens were cut parallel to the extrusion direction (WG).

3.3. Physical property measurements

The coefficient of thermal expansion (CTE) of H-451 specimens (stressed and unstressed controls) were measured using a silica push rod dilatometer over the temperature range 20–500 °C for the specimens irradiated at 600 °C, and 20–800 °C for specimens irradiated at 900 °C, under an inert cover gas.

4. Results and discussion

4.1. Compressive creep

The experimental (apparent) creep strain data from the ORR compressive creep series of experiments are reported in Figs. 2–5. In accord with the usual convention the apparent creep is taken to be the difference between the dimensional change of a stressed specimen and the unstressed control specimen. The apparent creep strain data up to a fluence of ~20% of the turn-around fluence is fitted to the linear visco-elastic creep law (Eq. (5)), with the zero dose creep strain being equal to (σ/E_0). The linear fit to the low dose data is shown in the Figs. 2–5 along with the corresponding equation

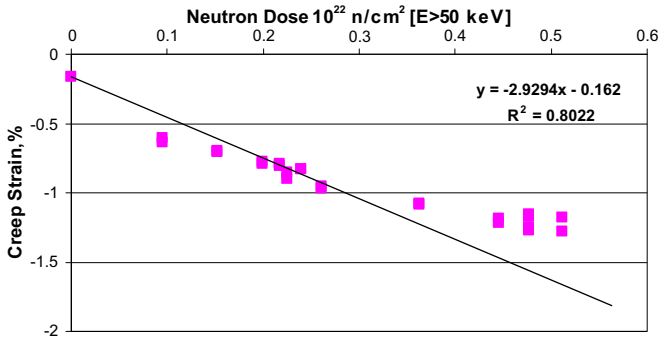

Fig. 2. Apparent creep strain for H-451 graphite irradiated at 600 °C and 13.8 MPa applied stress as a function of neutron dose.

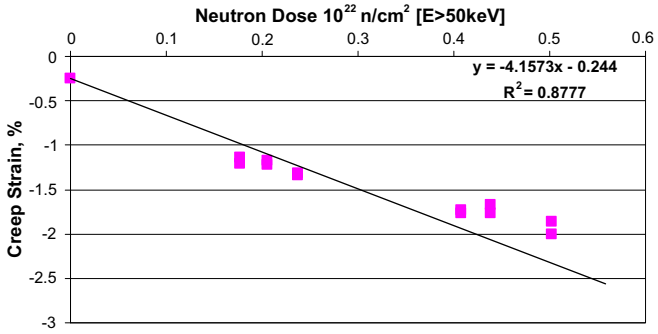

Fig. 3. Apparent creep strain for H-451 graphite irradiated at 600 °C and 20.7 MPa applied stress as a function of neutron dose.

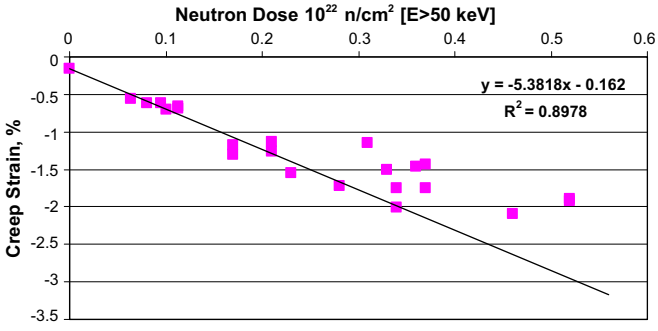

Fig. 4. Apparent creep strain for H-451 graphite irradiated at 900 °C and 13.8 MPa applied stress as a function of neutron dose.

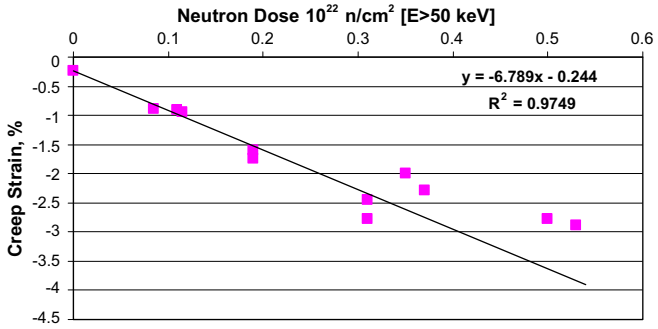

Fig. 5. Apparent creep strain for H-451 graphite irradiated at 900 °C and 20.7 MPa applied stress as a function of neutron dose.

and correlation coefficients. In each case the fit to the low dose data is fairly good, with correlation coefficients ~0.9.

Axial (WG) and radial (AG) creep strain data for H-451 irradiated at 900 °C under a applied compressive stress of 13.8 MPa are compared in Fig. 6. The creep strain data are similar at doses up to $\sim 0.5 \times 10^{22}$ n/cm^2, suggesting the creep rate is independent of preferred orientation in near-isotropic graphite.

The low dose creep strain data are represented by the linear law, and the calculated values of the steady state creep coefficient (k) are reported in Table 1. The units of k are given in % strain per unit dose [$E > 50$ keV] (directly from the data plots) and converted to the more familiar units of (cm^2/n Pa) [$E > 50$ keV].

From the low dose creep coefficient data in Table 1, k for H-451 graphite (mean of both stress levels) was found to be 0.205×10^{-30} cm^2/n Pa [$E > 50$ keV] at 600 °C and 0.360×10^{-30} cm^2/n Pa [$E > 50$ keV] at 900 °C. The creep coefficients for H-451 expressed

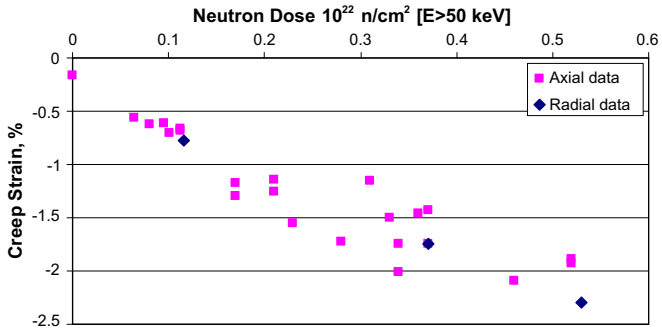

Fig. 6. Comparison of axial and radial orientation creep strain data for H-451 graphite irradiated at 900 °C under an applied stress of 13.8 MPa.

Table 1
Steady state creep coefficients (k) calculated from the low dose H-451 compressive creep strain data (Figs. 1–4)

Irradiation temperature (°C)	Applied compressive stress (MPa)	Creep coefficient, k (apparent creep strain (%)/ 10^{24} cm^2/n [$E > 50$keV])	Creep coefficient, k (10^{-30} cm^2/n Pa [$E > 50$keV])
600	13.8	2.93	0.21
600	20.7	4.16	0.20
900	13.8	5.38	0.39
900	20.7	6.79	0.33

in terms of creep strain per unit initial elastic strain, kE_0 (Eq. (6)) compare favorably with literature values. For H-451 these values are 1.8×10^{-21} cm^2/n [$E > 50$ keV] at 600 °C and 3.1×10^{-21} cm^2/n [$E > 50$ keV] at 900 °C (assuming $E_0 = 8.5$ GPa). Blackstone et al. [26] reported creep coefficients (kE_0) for pressed Gilso-carbon graphite irradiated ($E_0 = 10.5$ GPa) at 650 °C of 1.6 cm^2/n [$E > 50$ keV]. Veringa and Blackstone [27] reported creep data for Gilso-carbon graphite and extruded pitch coke graphite irradiated at 650 °C. The kE_0 values for the two graphite types were 2.1×10^{-21} cm^2/n [$E > 50$ keV] ($E_0 = 10.5$ GPa) and 1.75×10^{-21} cm^2/n [$E > 50$ keV] ($E_0 = 10$ GPa assumed here), respectively. The UK value for creep coefficient was reported to be 1.3×10^{-21} cm^2/n [$E > 50$ keV] for irradiation temperatures up to 500 °C [19]. Creep coefficients for IG-110, a fine-grain isotropic graphite, at irradiation temperatures between 900 and 1000 °C have been reported [11]. The coefficients (kE_0) ranged from 2.5 to 3.6×10^{-21} cm^2/n [$E > 50$ keV], in good agreement with the H-451 value at 900 °C of 3.1×10^{-21} cm^2/n [$E > 50$ keV].

While the low dose H-451 creep strain data are well represented by the linear creep law, with creep coefficients in broad agreement with the literature values, at higher neutron doses, especially at $T_{irr} = 900$ °C, the apparent creep strain data begins to deviate for the linear law (Figs. 2–5). Recently it has been recognized that creep strain produces significant modifications to the dimensional change component (behavior) of the stressed specimen compared to that of the control and that this must be accounted for in the correct evaluation of creep data. Changes in coefficient of thermal expansion due to irradiation and creep strain, and the crystal shape change parameter, X_T, must be evaluated with respect to irradiation dose in order to evaluate the correction to the true creep strain (Eq. (15)). The parameter X_T has been evaluated for H-451 at irradiation temperatures of 600 and 900 °C from dimensional change and Young's modulus data [28] and is shown in Figs. 7 and 8. The parameter X_T may be written as a quadratic function of neutron dose for irradiation temperatures of 600 and 900 °C, respectively

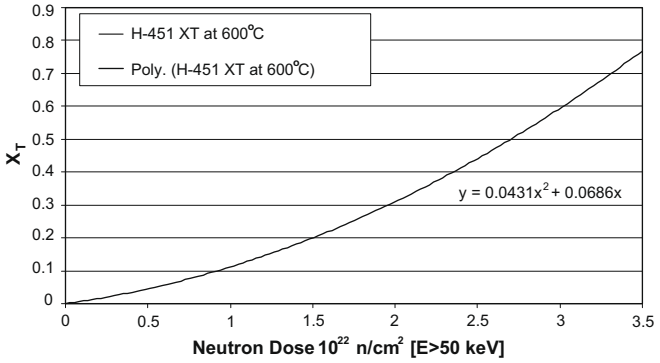

Fig. 7. The variation of X_T with neutron dose for H-451 at an irradiation temperature of 600 °C.

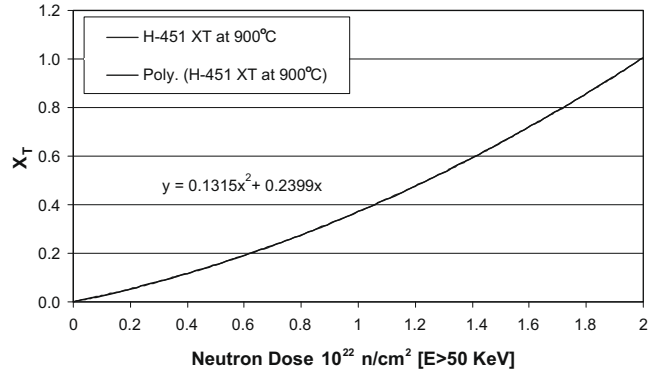

Fig. 8. The variation of X_T with neutron dose for H-451 at an irradiation temperature of 900 °C.

$$X_T = 0.0431\gamma^2 + 0.0686\gamma, \quad \text{and} \tag{16}$$

$$X_T = 0.1315\gamma^2 + 0.2399\gamma, \tag{17}$$

where γ is in units of 10^{22} n/cm^2 [$E > 50$ keV].

The effects of neutron irradiation to high doses (>4 × 10^{22} n/cm^2 [$E > 50$ keV]) on the CTE are shown for H-451 graphite in the WG direction at an irradiation temperature of 600 °C in Fig. 9. The CTE is observed to initially increase, reaching a maximum, and then decrease. Similar behavior has been reported for graphite grade N3M [29], grade ATR-2E [25] and grade IM1-24 [16]. The irradiated CTE behavior of H-451 at 600 °C can be described by the equation

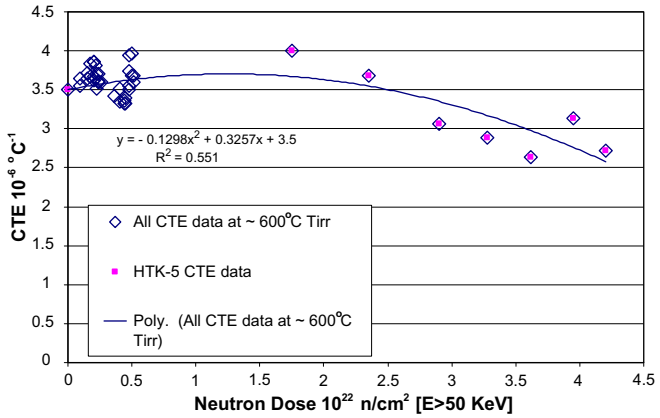

Fig. 9. Change of CTE with neutron irradiation for H-451 irradiated at 600 °C.

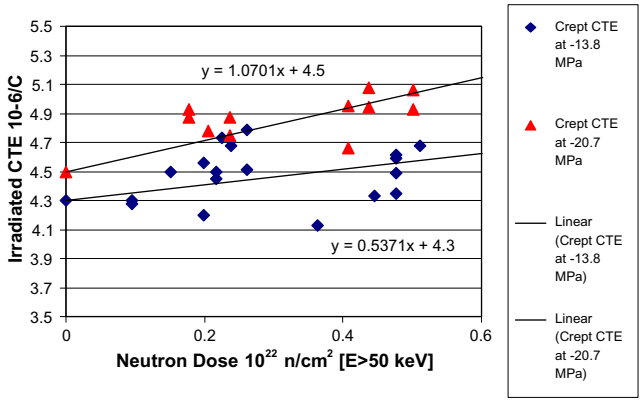

Fig. 10. Change in CTE with neutron dose and applied stress for H-451 graphite irradiated at 600 °C and at two applied compressive stress levels (13.8 and 20.7 MPa).

$$\alpha_x = 0.1298\gamma^2 + 0.3257\gamma + 3.5 \quad (10^{-6}\,^\circ\mathrm{C}^{-1}). \tag{18}$$

The effect of creep strain on the CTE of H-451 graphite at 600 °C is shown in Fig. 10 for applied stresses of 13.8 and 20.7 MPa. Over the limited neutron dose range for which compressive creep data is available the change in CTE is found to be represented by a linear relationship with neutron dose (Fig. 10)

$$\alpha'_x = 0.5371\gamma + 4.3 \quad (10^{-6}\,^\circ\mathrm{C}^{-1}), \tag{19}$$

at an applied stress of 13.8 MPa, and

$$\alpha'_x = 1.0701\gamma + 4.5 \quad (10^{-6}\,^\circ\mathrm{C}^{-1}), \tag{20}$$

at an applied stress of 20.7 MPa, where γ is in units of 10^{22} n/cm^2 [$E > 50$ keV]. The stressed CTE values at zero neutron dose are both greater than the unstressed value. This has been attributed to the closure of internal (Mrozowski) cracks due to compressive strain [17,30–32], such that the CTE at a compressive stress of 20.7 MPa would be expected to be greater than the CTE at 13.8 MPa.

The effects of neutron irradiation >1.5 × 10^{22} n/cm^2 [$E > 50$ keV] on the CTE are shown for H-451 graphite in the WG direction at an irradiation temperature of 900 °C in Fig. 11. The CTE is observed to initially increase, reaching a maximum, and then decrease and saturate, or possibly pass through a minimum. Similar behavior has been reported for graphite grades N3M [29], ATR-2E [25] and IM1-24 [16]. The CTE behavior at 900 °C is described by the equation

$$\alpha_x = 1.3882\gamma^3 - 4.0442\gamma^2 + 1.9309\gamma + 3.9 \quad (10^{-6}\,^\circ\mathrm{C}^{-1}), \tag{21}$$

where γ is in units of 10^{22} n/cm^2 [$E > 50$ keV].

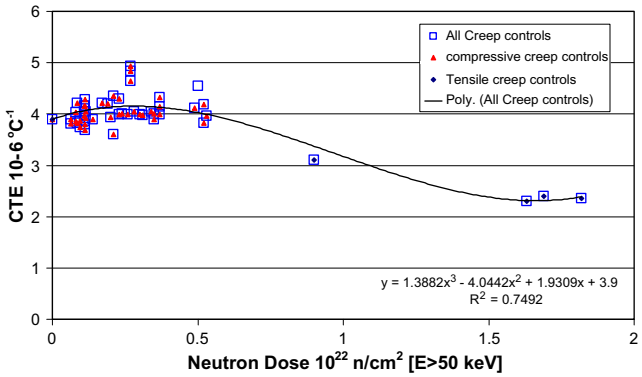

Fig. 11. Change in CTE with neutron dose for H-451 graphite irradiated at 900 °C.

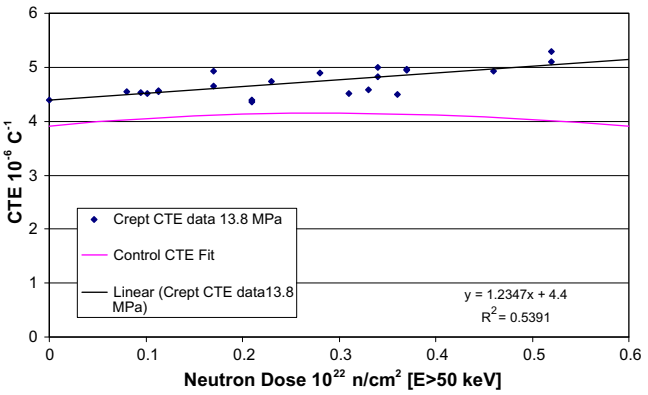

Fig. 12. Change in CTE with neutron dose and applied stress for H-451 graphite irradiated at 900 °C and an applied stress of 13.8 MPa.

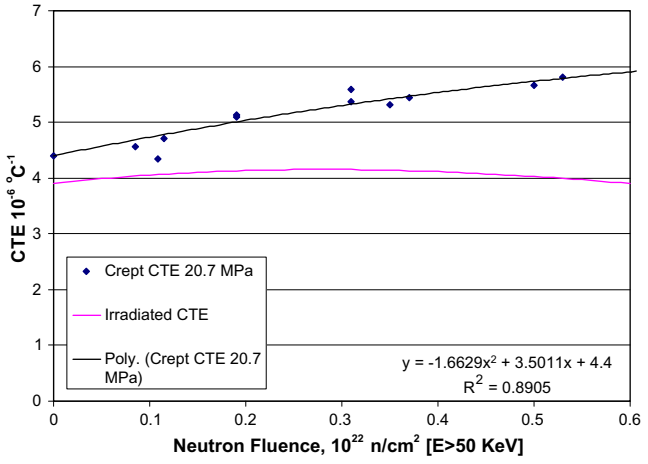

Fig. 13. Change in CTE with neutron dose and applied stress for H-451 graphite irradiated at 900 °C and an applied stress of 20.7 MPa.

The unirradiated ($\gamma = 0$) value of the CTE is greater at 900 °C (3.9×10^{-6} °C^{-1}) than at 600 °C (3.5×10^{-6} °C^{-1}) as would be expected [17,30–32] due to the thermal closure of Mrozowski cracks in the graphite.

The effect of creep strain on the CTE of H-451 graphite CTE at 900 °C is shown in Figs. 12 and 13 for applied stresses of 13.8 and 20.7 MPa, respectively. Over the limited neutron dose range for which compressive creep data is available the change in CTE is found to be represented by a linear relationship with neutron dose at an applied stress of 13.8 MPa (Fig. 12)

$$\alpha'_x = 1.2347\gamma + 4.4 \quad (10^{-6}\,^{\circ}\mathrm{C}^{-1}), \tag{22}$$

and a quadratic equation at an applied stress of 20.7 MPa

$$\alpha'_x = 1.6629\gamma^2 + 3.5011\gamma + 4.4 \quad (10^{-6}\,^{\circ}\mathrm{C}^{-1}), \tag{23}$$

where γ is in units of 10^{22} n/cm^2 [$E > 50$ keV].

At 900 °C and 20.7 MPa applied stress the relationship of CTE with neutron dose (and creep strain) is no longer linear. At higher irradiation temperatures the graphite is much closer to turnaround at the peak doses reported here. Consequently, the *c*-axis closure of aligned porosity is well advanced and the creation of new porosity due to mismatch of crystal strains has commenced. Gray [33] reported the change in CTE with dose for three different grades of graphite (AGOT, H-327, and POCO AXF-8Q) at stress levels of 6.9 MPa (1 ksi), 13.8 MPa (2 ksi), and 20.7 MPa (3 ksi). He observed that the CTE in the latter two grades tended to increase with creep strain to a maximum, and in some instances the CTE reversed. The dose range over which the CTE change may be assumed to be linear appears therefore to be limited, and is a function of the irradiation temperature and applied stress. The linear region with respect to neutron dose is reduced as the irradiation temperature and the magnitude of the applied stress increase.

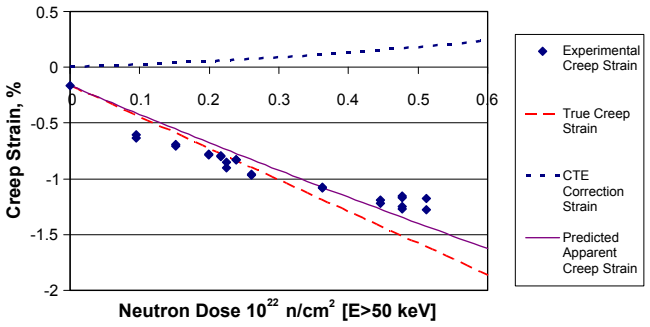

Fig. 14. Comparison of predicted apparent creep strain (from Eq. (15)) and the experimental creep strain data for irradiation creep at 600 °C under a compressive stress of 13.8 MPa. The true creep strain is calculated from Eq. (5).

The apparent (experimental) creep strain can now be predicted for each temperature and stress as a function of the irradiation dose from Eq. (15) by taking $(\alpha_c - \alpha_a) = 27 \times 10^{-6}$ °C^{-1} and applying Eqs. (16)–(23). Since the CTE change under a compressive stress is positive and the true creep is negative (compressive) the apparent creep strain will be less than the true creep strain. The predicted apparent creep strain is shown in Fig. 14 for irradiation creep at 600 °C under a compressive load of 13.8 MPa, and in Fig. 15 for irradiation creep at 600 °C under a compressive load of 20.7 MPa. Similarly, the predicted creep strain for an irradiation temperature of 900 °C and compressive stresses of 13.8 and 20.7 MPa are reported in Figs. 16 and 17, respectively.

The magnitude of the CTE correction strain (shown as the dotted line in Figs. 14–17) increases with increasing neutron dose, applied stress, and irradiation temperature. For example, at a neutron dose of 0.6×10^{22} n/cm^2 [$E > 50$ keV] the magnitude of the calculated correction at 600 °C increases from ~0.2% at 13.8 MPa to ~0.4% at 20.7 MPa. Similarly, the correction at 900 °C increases from ~0.9% at 13.8 MPa to ~1.4% at 20.7 MPa. In all cases the application of the calculated correction to the (linear) true creep strain results in an improved fit to the experimental data, as indicated by the solid line (predicted apparent creep strain) in Figs. 14–17.

The Kelly–Burchell model accounts for non-linearity by correcting the dimensional change component of the creep strain for the induced structural changes manifested through the observed

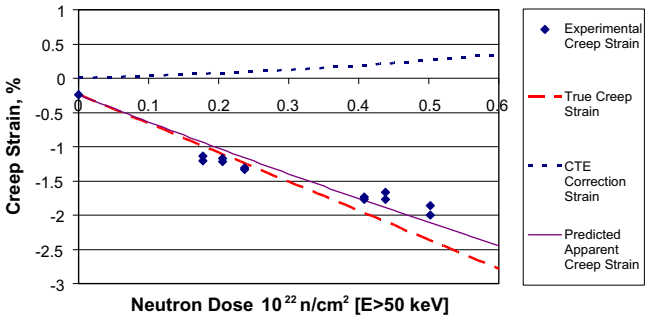

Fig. 15. Comparison of predicted apparent creep strain (from Eq. (15)) and the experimental creep strain data for irradiation creep at 600 °C under a compressive stress of 20.7 MPa. The true creep strain is calculated from Eq. (5).

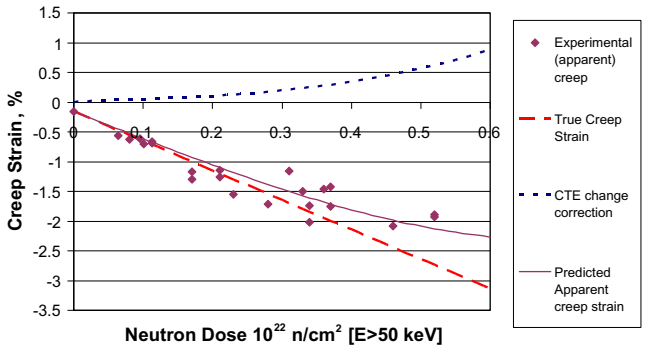

Fig. 16. Comparison of predicted apparent creep strain (from Eq. (15)) and the experimental creep strain data for irradiation creep at 900 °C under a compressive stress of 13.8 MPa. The true creep strain is calculated from Eq. (5).

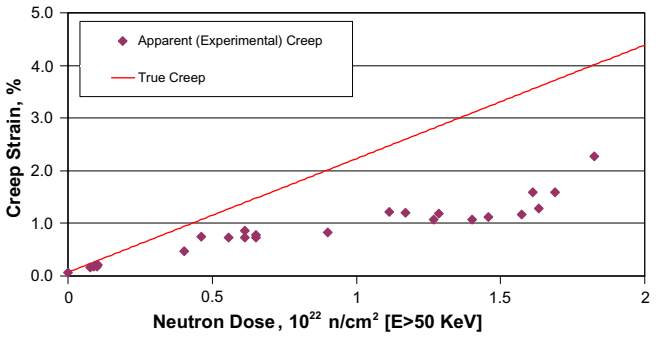

Fig. 18. A comparison of the experimental (apparent) tensile creep strain for an irradiation temperature of 900 °C and applied tensile stress of 6 MPa and the predicted true creep strain (from Eq. (5)).

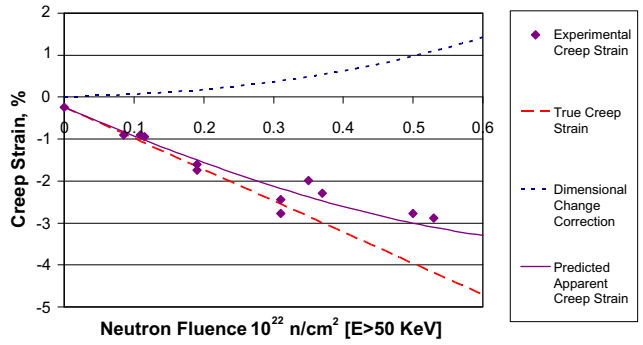

Fig. 17. Comparison of predicted apparent creep strain (from Eq. (15)) and the experimental creep strain data for irradiation creep at 900 °C under a compressive stress of 20.7 MPa. The true creep strain is calculated from Eq. (5).

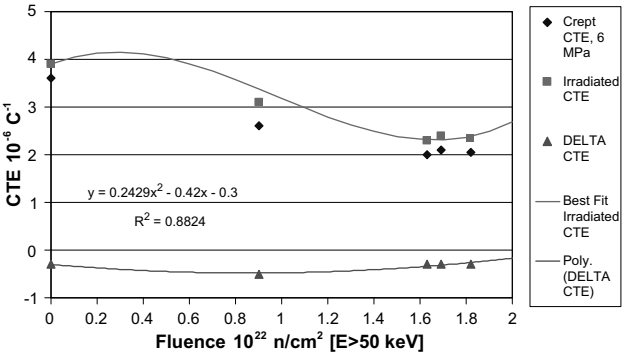

Fig. 19. The effect of neutron irradiation and irradiation creep on the CTE of H-451 graphite at an irradiation temperature of 900 °C. Also plotted is the change of CTE upon irradiation under stress (creep strain).

changes in CTE. This effect was noticeably more pronounced at 900 °C because the graphite is closer to turn-around at this temperature, because a larger fraction of the aligned porosity that accommodates the *c*-axis expansion is closed at the higher irradiation temperature. The model demonstrates the in-crystal creep (true creep) is linear, as postulated in the Kelly–Foreman model [5], but allows for changes in the graphite polycrystalline structure which manifest themselves as changes in the CTE in a crept specimen. This suggests the intermediate dose non-linearity is caused by changes in aligned porosity, both within the crystals and between the crystalline regions (domains) in the coke and binder. Such cracks are known to cause changes in the CTE under irradiation, and are thus likely to play a role in the polygrannular graphite creep mechanism.

4.2. Tensile creep

High dose apparent (experimental) creep strain data for H-451 graphite irradiated at 900 °C in the HFR at Petten are shown in Fig. 18 along with the calculated true creep strain (from Eq. (5)) setting k to 0.360×10^{-30} cm^2/n Pa [$E > 50$keV]. The departure from linearity is clearly evident, confirming the trend seen at lower dose in compression (especially at the higher irradiation temperature of 900 °C).

The effect of irradiation on the CTE of H-451 stressed (6 MPa tensile) and unstressed is shown in Fig. 19. There are very few data for the effects of tensile stress on CTE compared to the unstressed data base (represented by the solid line in Fig. 19). The CTE of the unstressed irradiated experimental controls are reasonably well represented by the solid line (taken for all the CTE data at 900 °C in Fig. 11). However, there are insufficient data to accurately define an irradiated stressed CTE curve. Also plotted in Fig. 19 are data for the change in CTE with creep ($\Delta\alpha$). These data show that the change in CTE with neutron dose (creep strain) is not linear over the reported dose range under tensile stress, as also observed for the higher compressive stress 900 °C CTE data.

The change in CTE is found to be well represented by the equation

$$\alpha'_x - \alpha_x = 0.2429\gamma^2 - 0.42\gamma - 0.3 \quad (10^{-6}\,^{\circ}\mathrm{C}^{-1}), \tag{24}$$

where γ is in units of 10^{22} n/cm^2 [$E > 50$ keV].

The CTE behavior reported here is in agreement with that reported by Gray [33] as discussed earlier. He reported the saturation and reversal of the CTE with increasing neutron dose (creep strain) at 800 °C.

The apparent (experimental) creep strain can now be calculated as a function of the irradiation dose from Eq. (15) by taking $(\alpha_c - \alpha_a) = 27 \times 10^{-6}\,^{\circ}\mathrm{C}^{-1}$ and applying Eqs. (17) and (24). Since the CTE change under a tensile stress is negative and the true creep is positive (tensile) the apparent creep strain will once again be less than the true creep strain. The predicted apparent creep strain is shown in Fig. 20 along with the experimental data. While there is reasonable agreement between the predicted apparent creep strain at low doses, the Kelly and Burchell creep model is not a good fit to the data at doses >0.5 $\times$ 10^{22} n/cm^2 [$E > 50$ keV].

Notably, the dimensional change correction term (dashed line in Fig. 20) increases in magnitude with neutron dose to a maximum at ~−1% at ~1.5 $\times$ 10^{22} n/cm^2 [$E > 50$ keV] and then reduces with increasing neutron dose.

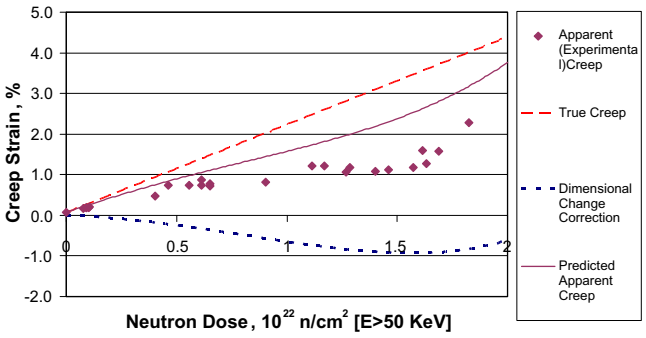

Fig. 20. Comparison of predicted apparent creep strain (from Eq. (15)) and the experimental creep strain data for irradiation creep at 900 °C under a tensile stress of 6 MPa. The true creep strain is calculated from Eq. (5).

5. General discussion

The poor performance of the Kelly and Burchell model (Eq. (15)) at predicting the high temperature (900 °C) and high dose 6 MPa tensile creep data (Fig. 20) suggests the model requires further revision. H-451 graphite irradiated at 900 °C goes through dimensional change turn-around in the dose range 1.3–1.5 × 10^{22} n/cm^2 [E > 50 keV]. This behavior is understood to be associated with the generation of new porosity due to the increasing mismatch of crystal strains. The model reported here accounts for this new porosity only to the extent to which it affects the CTE of the graphite, through changes in the aligned porosity. Since creep occurs at constant volume (up to moderate fluences) another pore related structural change must also occur.

Gray [33] observed at 550 °C the creep rate was approximately linear. However, at 800 °C he reported a marked non-linearity in the creep rate and the changes in CTE were significant. Indeed, for the two high density graphites Gray reports (H-337 and AXF-8Q) the 900 °C creep strain rate reverses. Gray postulated a creep strain limit to explain this behavior, such that a back stress would develop and cause the creep rate to reduce. Other workers have shown that a back stress does not develop [13]. However, Gray further argued that a creep strain limit is improbable since this cannot explain the observed reversal of creep strain rate. Note, a reversal of the creep rate is suggested by the 900 °C H-451 compressive creep strain data reported here and is clearly seen in the 900 °C tensile creep strain data reported here for H-451. Also, a creep strain limit would require that tensile stress would modify the onset pore generation behavior in the same way as compressive stress, because the direction of the external stress should be immaterial [33]. More recent data [25] and the behavior reported here shows that this is not the case. Gray suggests a more plausible explanation of his creep data is the onset of rapid expansion accelerated by creep strain, i.e., net pore generation begins earlier under the influence of a tensile applied stress. Indeed it has been observed [25] that compressive creep appears to delay the turn-around behavior.

In discussing possible explanations for his creep strain and CTE observations Gray noted that changes in the graphite pore structure that manifested themselves in changes in CTE did not appear to influence the creep strain at higher doses. The classical explanation of the changes in CTE invokes the closure of aligned porosity in the graphite crystallites. Further crystallite strain can only be accommodated by fracture. A result of this fracture is net generation of porosity resulting in a bulk expansion of the graphite. A requirement of this model is that the CTE should increase monotonically from the start of irradiation. A more marked increase in CTE would be seen when the graphite enters the expansion phase (i.e., all accommodating porosity filled). The observed CTE behavior reported here and in Gray's work [33] does not display this second increase in CTE, thus the depletion of (aligned) accommodation porosity is not responsible for the early beginning of expansion behavior.

The observation by Gray [33] and Kennedy [14] that creep occurs at near constant volume (up to moderate fluences) indicates that creep is not accompanied by a net reduction of porosity compared to unstressed graphite, but this does not preclude that stress may decrease pore dimensions in the direction of the applied stress and increase them in the other, i.e., a re-orientation of the pore structure. Pore re-orientation could effectively occur as the result of a mechanism of pore generation where an increasing fraction of the new pores are not well-aligned with the crystallites basal planes (and thus would not manifest themselves in CTE behavior) accompanied with the closure of pores aligned with the basal planes.

Kelly and Foreman [5] report that their proposed creep mechanism would be expected to break down at high doses and temperatures, and thus deviations from the linear creep law (Eq. (5)) are expected. They suggest this is due to (i) incompatibility of crystal strains causing additional internal stress and an increasing creep rate, (ii) destruction of interstitial pins by diffusion of vacancies (thermal annealing of vacancies in addition to irradiation annealing), and (iii) pore generation due to incompatibility of crystal strains. Here we postulate that this pore generation can manifest itself in two ways (a) changes in CTE with creep strain – thus pores aligned parallel to the crystallite basal planes are affected by creep strain, and (b) at high doses pore generation or perhaps pore re-orientation, under the influence of stress that must be accounted for in the prediction of high neutron dose creep behavior.

Brocklehurst and Brown [13] report on the annealing behavior of specimens that had been subjected to irradiation under constant stress and sustained up to 1% creep strain. They observed that the increase in creep strain with dose was identical in compression and tension up to 1% creep strain, and that the CTE was significantly affected in opposite directions by compressive and tensile creep strains. Irradiation annealing of the crept specimens caused only a small recovery in the creep strain, and therefore provided no evidence for a back stress in the creep process, which has implications for the in-crystal creep mechanism. Thermal annealing also produced a small recovery of the creep strain at temperatures below 1600 °C, presumably due to the thermal removal of the irradiation induced defects responsible for dislocation pinning. Higher temperature annealing produced a further substantial recovery of creep strain. Most significantly, Brocklehurst and Brown [13] reported the complete annealing of the creep induced changes in CTE, in contrast to the total creep strain, where a large fraction of the total creep strain is irrecoverable and has no effect on the thermal expansion coefficient. Brocklehurst and Brown [13] discuss two interpretations of their results, but report that neither is satisfactory. One interpretation requires a distinction between changes in porosity that affect the CTE and changes in porosity affecting the elastic deformation under external loads, i.e., two distinct modes of pore structure changes due to creep in broad agreement with the mechanism proposed here.

The modified Simmons model [20,21] for dimensional changes (Eq. (8)) and for dimensional changes of a crept specimen (Eq. (10)) both have terms for pore generation which are currently neglected. It now appears necessary to modify the current creep model (Eq. (15)) to account for this effect of creep strain on this phenomena, i.e., we need to evaluate and take account of the terms F_x and F'_x and include the term $(F'_x - F_x)$ in Eq. (15). Such a term should account for pore generation and/or re-orientation caused by fracture when incompatibilities in crystallite strains become excessive. This is the focus of our current work and will be reported soon.

6. Conclusions

The Kelly and Burchell creep model previously applied to compressive creep data for H-451 graphite irradiated at 900 °C (13.7 and 20.8 MPa) has been extended to compressive creep data for H-451 irradiated at 600 °C (13.7 and 20.8 MPa). The basis of the creep model was discussed and the experimental data required to evaluate the terms in the creep model were reported and discussed. The model, which corrects the true (crystal) creep strain for the effect of creep on the dimensional change component of the creep specimen, is shown to be a good fit to the experimental compressive creep strain data. Significantly, the magnitude of the dimensional change correction increases with dose, applied stress, and irradiation temperature, over the dose range of the compressive creep data. The dimensional change correction applied in the model is calculated from the change in CTE between the stressed and unstressed specimen. The CTE change was observed to be approximately linear over the dose range reported for the 600 °C data at both compressive stresses, and at 900 °C at the lower compressive stress (13.8 MPa). However, at the higher applied compressive stress level (20.7 MPa) at 900 °C the change in CTE was found to be non-linear, with the rate of increase in CTE decreasing with increasing dose, i.e., CTE appears to saturate with dose in this case (over the range reported). The observed CTE behavior with dose and creep strain was explained in terms of the closure of aligned porosity (which is known to affect the dilation behavior), and at higher doses (post turn-around) the generation of additional porosity that affects the dilatational behavior.

Creep strain data for H-451 graphite irradiated at 900 °C under a tensile stress of 6 MPa was also reported, along with the required experimental data to evaluate the terms in the creep model. The magnitude of the dimensional change correction increases with dose and then decreases. The model is shown to inadequately represent the high dose (post volume turn-around) H-451 creep strain data.

It was postulated that the effects of porosity on the creep strain must be further accounted for. Such a term should account for pore generation and/or re-orientation caused by fracture when incompatibilities in crystallite strains become excessive. Currently the Kelly and Burchell model only accounts for pore generation to the extent that it changes CTE during creep. Consequently, a further correction to the model is required to account for additional pore structure changes. Support for the possible role of pore structure changes from the literature was reviewed and discussed. An additional pore structure correction is required because the creep mechanism due to Kelly and Foreman, which underpins the current model, is a graphite crystal deformation mechanism and takes no account of the interaction of porosity in the graphite creep deformation mechanism. It is suggested that the pore generation term in the modified Simmons model of graphite dimensional change should be evaluated for crept and control samples. Current work at ORNL is directed toward this goal.

Acknowledgements

This work is sponsored by the US Department of Energy, Office of Nuclear Energy Science and Technology under contract DE-AC05-00OR22725 with Oak Ridge National Laboratory, managed by UT-Battelle, LLC.

References

[1] T. Burchell, R. Bratton, Graphite Irradiation Creep Capsule AGC-1 Experimental Plan, ORNL/TM-2005/505, May 2005.
[2] J. McDufee, T.D. Burchell, D.W. Heartherly, K.R. Thoms, J. Nucl. Mater. 381 (2008) 119.
[3] T.D. Burchell, in: T.D. Burchell (Ed.), In Carbon Materials for Advanced Technologies, Published Elsevier Science, 1999, p. 429. Chapter 13.
[4] G.B. Engle, W.P. Eatherly, High Temp.-High Press. 1 (1972) 119.
[5] B.T. Kelly, A.J.E. Foreman, Carbon 12 (1974) 151.
[6] D.G. Martin, R.W. Henson, Philos. Mag. 9 (1967) 659.
[7] D.G. Martin, R.W. Henson, Carbon 5 (1967) 313.
[8] B.T. Kelly, J.H.W. Simmons, J.H. Gittus, P.T. Nettley, in: Proceedings of the Third UN Conference on Peaceful Uses of Atomic Energy, 10 339, Published International Atomic Energy Agency, Vienna, 1972.
[9] B.T. Kelly, J.E. Brocklehurst, J. Nucl. Mater. 65 (1977) 79.
[10] G. Jouquet, G. Kleist, H. Veringa, J. Nucl. Mater. 65 (1977) 86.
[11] T. Oku, M. Eto, S. Ishiyama, J. Nucl. Mater. 172 (1990) 77.
[12] H. Hansen, R. Loelgen, M. Cundy, J. Nucl. Mater. 65 (1977) 148.
[13] J.E. Brocklehurst, R.G. Brown, Carbon 7 (1969) 487.
[14] C.R. Kennedy, in: Conf 901178-1, ORNL, 1990.
[15] T. Oku, M. Eto, S. Ishiyama, J. Nucl. Sci. Technol. 24 (8) (1987) 670.
[16] Tatsuo Oku, Masahiro Ishihara, Nucl. Eng. Des. 227 (2004) 209.
[17] J.E. Brocklehurst, B.T. Kelly, Carbon 31 (1) (1993) 155.
[18] B.T. Kelly, Carbon 30 (3) (1992) 379.
[19] B.T. Kelly, T.D. Burchell, Carbon 32 (1994) 119.
[20] J.W.H. Simmons, Radiation Damage to Graphite, Pergamon, London, 1961.
[21] B.T. Kelly, W.H. Martin, P.T. Nettley, Philos. Trans. Roy. Soc. A 260 (1966) 37.
[22] R.L. Senn, W.H. Cooke, J.A. Conlin, W.P. Eatherly, J. Nucl. Mater. 65 (1976) 96.
[23] A.S. Mobasheran, PhD Thesis, University of Tennessee, 1990.
[24] C.R. Kennedy, M. Cundy, G. Kliest, in: Proceedings of CARBON '88, Newcastle upon Tyne, UK, Published Institute of Physics, London, 1985.
[25] G. Haag, Report No. Jul-4183, Properties of ATR-2E Graphite and Property Changes due to Fast Neutron Irradiation, Published FZ-J, Germany.
[26] R. Blackstone, L.W. Graham, M.R. Everett, in: Proceedings of the 9th Biennial Conference on Carbon, Boston College, MA, 16–20 June 1969.
[27] H.J. Veringa, R. Blackstone, Carbon 14 (1976) 279.
[28] B.T. Kelly, T.D. Burchell, Carbon 32 (1994) 449.
[29] T.D. Burchell, W.P. Eatherly, J. Nucl. Mater. 179–181 (1991) 205.
[30] S.D. Preston, B.J. Marsden, Carbon 44 (2006) 1250.
[31] B.T. Kelly, Physics of Graphite, Published Applied Science, 1981.
[32] S. Mrozowski, in: Proceedings of the First and Second Conference on Carbon, Buffalo, 1953 and 1955, University of Buffalo Press, Buffalo, New York, 1956.
[33] W.J. Gray, Carbon 11 (1973) 383.